Fluidization by lift of 300 circular particles in plane Poiseuille flow by direct numerical simulation

H.G. Choi and Daniel D. Joseph

Department of Aerospace Engineering & Mechanics
107 Akerman Hall
110 Union Street SE
University of Minnesota
Minneapolis, MN 55455

Abstract

We study the transport of a slurry of heavier than liquid circular particles in a plane pressure driven flow in a direct simulation. The flow is calculated in a periodic domain containing 300 circular particles. The study leads to the concept of fluidization by lift in which all the particles are suspended by lift forces against gravity perpendicular to the flow. The study is framed as an initial value problem in which a closely packed cubic array of particles resting on the bottom of the channel are lifted into suspension. All the details of the flow are resolved numerically without model assumptions. The fluidization of circular particles first involves bed inflation in which liquid is driven into the bed by high pressure at the front and low pressure at the back of each circle in the top row. This kind of bed inflation occurs even at very low Reynolds numbers but it takes more time for the bed to inflate as the Reynolds number is reduced. It appears that the bed will not inflate if the shear Reynolds number is below the critical value for single particle lift-off. The flows with a single particle are completely determined by a shear Reynolds number and a gravity parameter when the density ratio and aspect ratio parameters are specified. In the multi particle case the volume fraction and distribution also matters. The transition to a fully fluidized slurry by waves is discussed.

An analytical model of the steady motion of a single particle dragged forward in a Poiseuille flow is derived and compared with a simulation. The undisturbed fluid velocity is always larger than the particle velocity producing a fluid *hold-up*. The effect of the hold-up in the many particle case is to greatly reduce the velocity of the mixture which may be described by a two-fluid model in which the solid laden mixture is regarded as a second fluid with effective properties.

1 Introduction

The problem of transport of particles by fluids in horizontal conduits and pipes is of considerable scientific and industrial importance and is the focus of this paper. This problem arises in the transport of coal-water slurries, in the removal of drill cuttings in drilling of horizontal oil wells and in proppant transport in hydraulically fractured rock in oil and gas bearing reservoirs, to name a few. The central unsolved fluid dynamics problem arising in these applications is the

problem of fluidization by lift. The problem of fluidization by lift can be well framed in the problem of hydraulic fracturing.

Hydraulic fracturing is a process often used to increase the productivity of a hydrocarbon well. A slurry of sand in a highly viscous, sometimes elastic, fluid is pumped into the well to be stimulated at sufficient pressure to exceed the horizontal stresses in the rock at reservoir depth. This opens a vertical fracture, some hundreds of feet long, tens of feet high, and perhaps an inch in width, penetrating from the well bore far into the pay zone. When the pumping pressure is removed, the sand acts to prop the fracture open. Productivity is enhanced because the sand-filled fracture offers a higher-conductivity path for fluids to enter the well than through the bulk reservoir rock, and because the area of contact for flow out from the productive formation is increased. It follows that a successful stimulation job requires that there be a continuous sand-filled path from great distances in the reservoir to the well, and that the sand is placed within productive, rather than non-productive, formations.

In a slot problem a particle laden (say 20% solids) fluid is driven by a pressure gradient and the particles settle to the bottom as they are dragged forward. Sand deposits on the bottom of the slot; a mound of sand develops and grows until the gap between the top of the slot and the mound of sand reaches an equilibrium value; this value is associated with a critical velocity. The velocity in the gap between the mound and the top of the slot increases as the gap above the mound decreases. For velocities below critical the mound gets higher and spreads laterally; for larger velocities sand will be washed out until the equilibrium height and velocity are reestablished (see figure 1). The physical processes mentioned here are *settling* and *washout*. Washout could be by sliding and slipping; however, a more efficient transport mechanism is by *advection after suspension* which we studied by direct simulation.

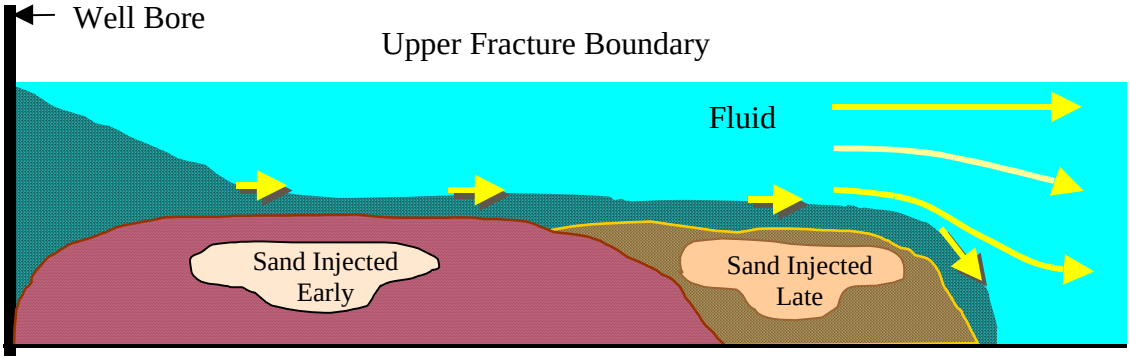

Figure 1. Sand transport in a fractured reservoir (after Kern, Perkins and Wyant [1959]).

In fluidized beds and sedimentation columns in which particles are in a balance of buoyant weight and drag, the cooperative effects of other nearby particles enter strongly into the dynamics. These effects are described by theories of hindered motion. There is a very definite relation between the fluidization by drag of one single isolated particle and the fluidization of a particle in a swarm of other particles; for example, the Richardson-Zaki correlation [1954]. Analogous ideas must come into play in problems of slurries which are fluidized by lift rather than by drag; hindered motion effects involving the effective viscosity and the effective density of a suspension and other cooperative effects surely enter here but are not well understood.

The problem of lift on a single particle has been treated by many authors in the low Reynolds number limit. Even in the much better understood subject of drag on a single particle, say a drag on a sphere, there are no first principle formulas and empirical relations must be used. The problem of lift on a single circular particle in Poiseuille flow at finite Reynolds numbers has been studied in direct numerical simulation by N. Patankar, Huang, Ko and Joseph [2000]; this paper has a discussion of previous work which will not be repeated here.

The aforementioned study of N. Patankar *et al.* is based on an ALE method using body-fitted unstructured finite element grids very closely related to the numerical method introduced by Choi [2000] and used here. A Chorin [1968] type fractional step scheme for particulate flows is introduced in the approach by Choi [2000].

Using the ALE particle mover, N. Patankar *et al.* did *lift-off* and *slip-velocity* fluidization studies in Newtonian and viscoelastic fluids. A heavier than liquid particle is resting on the bottom of a channel in the presence of a shear (Poiseuille) flow. At a certain critical speed, depending on the weight and diameter of the particle, the fluid properties, and the aspect ratio of the channel, the particle rises from the wall to an equilibrium height at which the buoyant weight just balances the upward thrust of fluid forces. The values of the particle velocity, the angular velocity of the particle, the slip velocity and the angular slip velocity at equilibrium together with the values of the relevant dimensionless parameters were tabulated.

In section 3 we shall do single particle lift-to-equilibrium studies at larger Reynolds numbers than N. Patankar *et al.* [2000] had done previously; the rise and other equilibrium properties are not smooth functions of the prescribed pressure gradient; we find instability and hysteresis which N. Patankar et al. have identified as a double turning point solutions. The existence of multiple steady solutions for single particle lifting may have important implications for slurries. Certainly such considerations are not found in models of solid-liquid flow and it is necessary to visit this question in the future.

In section 4 we carry out studies of fluidization by lift of 300 particles in the same plane Poiseuille flow used to study the lift to equilibrium of a single particle. The computation is carried out in a long periodic domain in which the volume fraction of solid circles ranges roughly between 78 % and 31%. The study is framed as an initial value problem in which a closely spaced cubic array of particles resting on the bottom of the channel are lifted into suspension.

The following picture emerges from this study. At early times the top of the array is only slightly disturbed; since the cubic crystal array is not tightly packed the top layers move forward relative to the bottom. The lifting of particles out of suspension is accomplished by a pressure mechanism clearly revealed by the simulation; liquid is driven into the bed by high pressure at the front and low pressure at the back of each circle in the top row. The particles are dislodged by this pressure mechanism. At higher Reynolds numbers single particles are thrown out of the bed in a manner resembling saltation. Typically isolated particles will fall back into the bed because the drag on an isolated particle is less than when it is among many. The permanent lifting of more particles of the bed takes shape in the formation of waves, which resemble water waves. The wave amplitude grows as the pressure gradient and flow speed increase; particles are levitated out of the bed and the levitated particles form a fluidized suspension over a basically fixed bed. This can be described as bed erosion. It is possible to erode the whole bed and fluidize

all of the particles by lift if the pressure gradient is high enough and the bed depth small enough. The wave amplitude decreases when the particles are fully fluidized.

The evolution to full fluidization is associated with a transition from a basically vertical stratification of dynamic pressure to a basically horizontal stratification of dynamic pressure. The final state of full fluidization is not steady. Internal pressure waves which propagate horizontally are associated with the propagation of particle depleted regions which could be described as an internal wave of the volume fraction.

A single heavier than liquid particle will not lift off at low pressure gradients; the particle slides and rolls on the wall; lift-off to equilibrium occurs at critical values. In the fluidized suspension we can track the evolution of the rise of the mass center of the particles. The final state of full fluidization can be determined as the leveling off of the rise of the mass center curve. The mass center did not rise even after a long computation when the pressure gradient was below the one critical for the rise of a single particle.

2 Equations of motion and scaling parameters

We use the same scales and equations as Patankar *et al* [2000]; (length, time, velocity, stress) = $(d, \dot{\gamma}_w^{-1}, \dot{\gamma}_w d, \eta\dot{\gamma}_w)$ and find that the governing dimensionless equations for slurry flow of 300 circular particles can be written as

$$R\left[\frac{\partial \mathbf{u}}{\partial t} + \mathbf{u}\cdot\nabla\mathbf{u}\right] = -\nabla p + \frac{2d}{W}\mathbf{e}_x + \nabla^2\mathbf{u} \quad \text{fluid} \tag{2.1}$$

$$\left.\begin{aligned} \frac{\rho_p}{\rho_f} R\frac{d\mathbf{U}}{dt} &= -G\mathbf{e}_y + \frac{2d}{W}\mathbf{e}_x + \frac{2}{\pi}\int_0^{2\pi}\cdot\boldsymbol{\sigma}\, d\theta \\ \frac{\rho_p}{\rho_f} R\frac{d\boldsymbol{\Omega}}{dt} &= \frac{16d}{\pi}\int_0^{2\pi}\mathbf{e}_r \wedge \boldsymbol{\sigma}\, d\theta \end{aligned}\right\} \text{ solid} \tag{2.2}$$

where $\mathbf{e}_r$ is the radial unit vector from the center of the circle; $\boldsymbol{\sigma} = -p\mathbf{e}_r + 2\mathbf{D}[y]\bullet\mathbf{e}_r$ is the stress vector,

$$\left.\begin{aligned} R &= \rho_f \dot{\gamma}_w d^2/\eta \quad \text{shear Reynolds number} \\ G &= \frac{\rho_p - \rho_f}{\eta\dot{\gamma}_w} gd \quad \text{gravity parameter.} \end{aligned}\right\} \tag{2.3}$$

Instead of R and G we may use the product

$$R_G = RG = \frac{U_s d\rho_f}{\eta g U_s} = \frac{d^2\left(\rho_p - \rho_f\right)g}{\eta} \tag{2.4}$$

and ratio

$$\frac{R}{G} = \frac{d\,\dot{\gamma}_w^{\,2}}{\left(\frac{\rho_p}{\rho_f} - 1\right) g} \tag{2.5}$$

The sedimentation Reynolds number R_G does not depend on $\dot{\gamma}_w$, and the generalized Froude number R/G does not depend on the viscosity η.

Adherence boundary conditions are prescribed also at the boundary of each circle

$$\mathbf{u} = \mathbf{U} + \boldsymbol{\Omega} \wedge \mathbf{e}_r d \tag{2.6}$$

When, as in a slurry, there are many particles the number N and places of N boundaries enter into the problem description. In the present case, 300 is the number and the places of these 300 particles evolve as part of the solution. We have similarity then for all evolution problems for which N, d/W, ρ_p/ρ_f, R, G are identical. In fact, the density ratio ρ_p/ρ_f enters only in (2.2) as the coefficient of the acceleration terms, hence does not enter for steady flow. Though steady flows of a single particle do occur and were studied by Patankar *et al* [2000], steady flow of many particles do not appear to occur in the multiple particle case after lift off; it is possible that the accelerations are small, however after the bed has fully expanded.

3 Problem formulation

The problem to be considered is the levitation of particles of diameter d in a plane Poiseuille flow in a horizontal channel of width W as shown in figure 2.

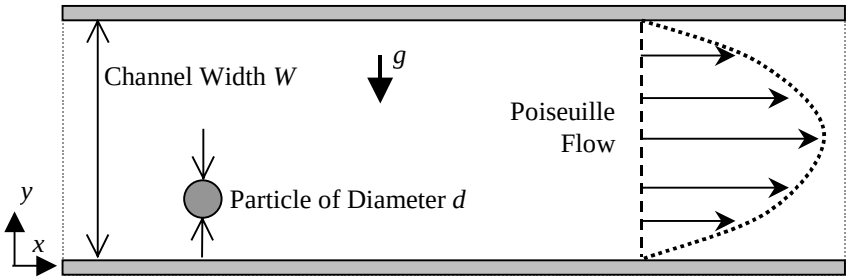

Figure 2. Levitation of heavier than liquid particle in a plane Poiseuille flow. The disturbed flow is periodic with period L.

The undisturbed Poiseuille flow is given by

$$\begin{aligned} U(y) &= 4U_m \frac{y}{W}\left(1-\frac{y}{W}\right), \\ U_m &= U\left(\frac{W}{2}\right) = \frac{W^2 \overline{p}}{8\eta}, \\ \dot{\gamma} &= \frac{du}{dy}, \\ \dot{\gamma}_w &= \frac{4U_m}{W} = \frac{W\overline{p}}{2\eta} \end{aligned} \tag{3.1}$$

The presence of particles disturbs the Poiseuille flow. It is assumed that the disturbance flow, satisfying equations (2.10) is periodic with period L. This periodicity is strictly enforced in the computation by the construction of a periodic mesh. The solution of the disturbance flow depends on L, but only weakly for large L. We used

$L = 22d$ for single particle,

$L = 63d$ for 300 particles.

All the calculations were carried out in dimensional variables using CGS units. The height of the channel is $W = 12d$ and $d = 1$ cm. The particle density is $\rho_p = 1.01\ \rho_f$ and the fluid density $\rho_f = 1$ gm/cc. We did calculations for three different viscosities $\eta = 1$, 0.2 and 0.01 poise, from light oil to water. For each η, the calculations were done for different pressure gradient $\overline{p}$ in dynes/ cm^2.

The results of calculations in dimensional variables may be generalized by post processing. In the present case ρ_p/ρ_f, d/W, d/L and the number of particles in a cell are fixed and flows are completely determined by the shear Reynolds number R and gravity number G given by (2.11).

4 Fluidization of 300 circular particles

Here we study the problem of lift of 300 solid circles in plane Poiseuille flow (figure 2) when $\rho_p = 1.01\ \rho_f$, $\rho_f = 1$ gm/cc, $W = 12d$, $d = 1$ cm for viscosities $\eta = 1$, 0.2 and 0.01 poise (from light oil to water). The calculations are carried out in a periodic domain $L = 63d$ which is long enough to contain four or more of the waves of pressure which characterize fully fluidized beds of 300 particles. The period of the waves does not depend on the period of the computational cell provided that the cell contains more than three waves. Initially the circles are arranged in a square lattice in which the particles do not touch; they are separated by 0.05 cm when $\eta = 1$ and $\eta = 0.2$ poise, and by 0.1 cm when $\eta = 0.01$ poise. The height of the array is 5.25 cm and 5.35 cm.

Initially the particle array is at rest and the fluid above is a developed Poiseuille flow; this kind of initial condition causes a faster saltation type of lift, like a dust storm in a sudden wind. The same final rise height can be obtained from different initial conditions.

We recall that the results of calculations may be generalized by computing the values of the shear Reynolds number $R = \dot{\gamma}_w d^2 / \nu$ and the gravity number $G = d\left(\rho_p - \rho_f\right)g / \dot{\gamma}_w \eta$ defined in (2.11). The value $R_G = RG = \rho_f d^3 \left(\rho_p - \rho_f\right) g / \eta^2 = 9.81/\eta^2$ is independent of $\dot{\gamma}_w$. The running index in our calculation is the pressure gradient $\overline{p}$; given η this determines $R = \rho d^2 W\, \overline{p} / 2\eta^2 = 6\overline{p} / \eta^2$.

Case 1: η = 1 poise, R_G = 9.81

Figure 3 shows the height of the center of gravity of the 300 particles as a function of $R = 6\overline{p}$. We say that the bed height has attained its final fully fluidized value when the rise curve levels off. Average values of the bed height $\overline{H}$, the average velocity $\overline{U}$cm/sec and angular velocity $\overline{\Omega}$sec^{-1} at full inflation are given in Table 1. The time taken for the center of gravity to reach its fully fluidized value increases as the Reynolds number R decreases. Figure 4, 5, 6 and 10 show snapshots of the evolution of the bed to full fluidization at values of R, G, given in the caption to figure 3.

Animations for these snapshots can be found at our URL *http://www.aem.umn.edu/Solid-Liquid_Flows*. The snapshots are decorated by shades of gray coded to reveal the distribution of dynamic pressure ($\overline{p}$ in equation (3.1)); dark means low pressure. Figures 8 and 9 give graphs of the pressure at different cross-sections of the channel for R = 120 at an early time t = 0.9 sec and when the suspension is fully fluidized at t = 27 sec. At early times the pressure is stratified vertically, but not horizontally; at the later time the pressure is stratified horizontally and not vertically.

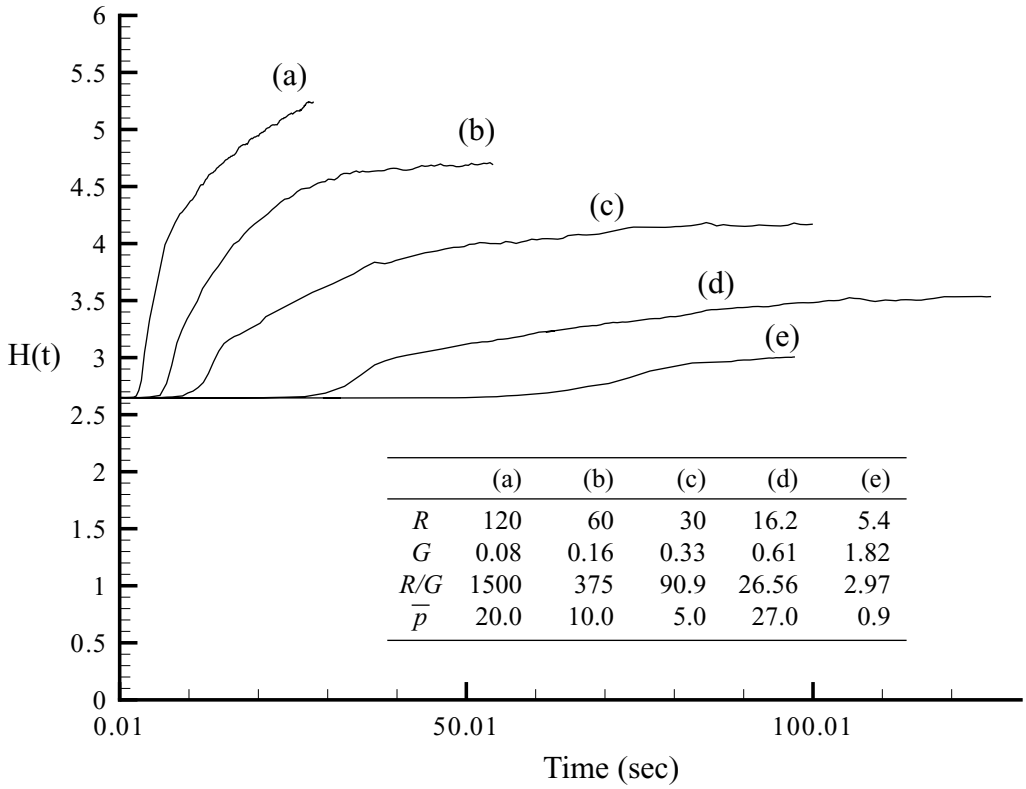

	(a)	(b)	(c)	(d)	(e)
R	120	60	30	16.2	5.4
G	0.08	0.16	0.33	0.61	1.82
R/G	1500	375	90.9	26.56	2.97
$\overline{p}$	20.0	10.0	5.0	27.0	0.9

Figure 3. Rise curves for the center of gravity of 300 circular particles fluidized by lift (fluid viscosity = 1.0 poise, G *= 9.81/*R*). The time scale for the slow rise at* $\overline{\text{p}}$ *= 0.9 dynes/cm^2 has been compressed by 2; the real time corresponding say, to 50.01 is 100.02 sec. The bed is said to be fully fluidized when the rise curves level off. The time to full fluidization is longer when the Reynolds number is smaller.*

Table. 1 Data for the forward motion of a fluidized suspension of 300 particles after the bed has fully inflated and the average height $\overline{H}$ *of all particles has stopped increasing* $(\eta = 1.0)$. $\overline{H} = \overline{H}_o = 2.65d$ *at t=0.* $\overline{U}$ *and* $\overline{\Omega}$ *are the average velocity and angular velocity of the particles.*

R	G	$\overline{p}$	$\overline{H}$	$\overline{U}$	$\overline{\Omega}$
5.4	1.82	0.9	3.01	2.09	0.28
16.2	0.61	2.7	3.54	9.55	1.026
24	0.41	4.0	4.00	18.62	1.75
30	0.33	5.0	4.17	25.63	2.25
60	0.16	10.0	4.69	55.60	3.85
120	0.08	20.0	5.24	119.76	4.90

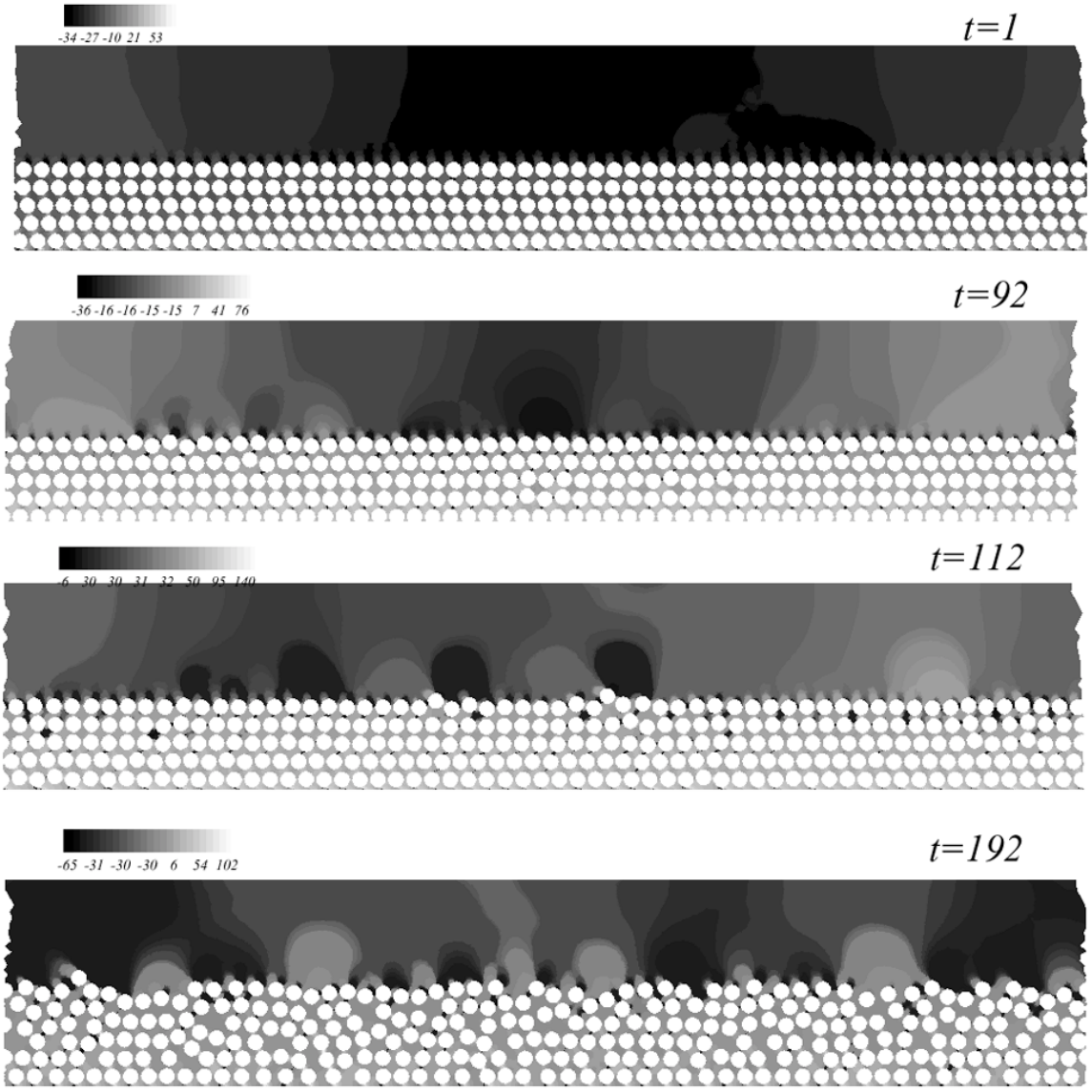

*Figure 4. Snapshots of the fluidization of lift of 300 circular particles ρ_p = 1.01 g/cm^3 when η = 1 poise (*R = 5.4, G = 1.82*). The flow is from left to right. The gray scale gives the pressure intensity and dark is for low pressure. At early times particles are wedged out of the top layer by high pressure at the front and low pressure at the back of each and every circle in the top row. The vertical stratification of pressure at early times develops into a "periodic" horizontal stratification, a propagating pressure wave. The final inflated bed has eroded, rather tightly packed at the bottom with fluidized particles at the top.*

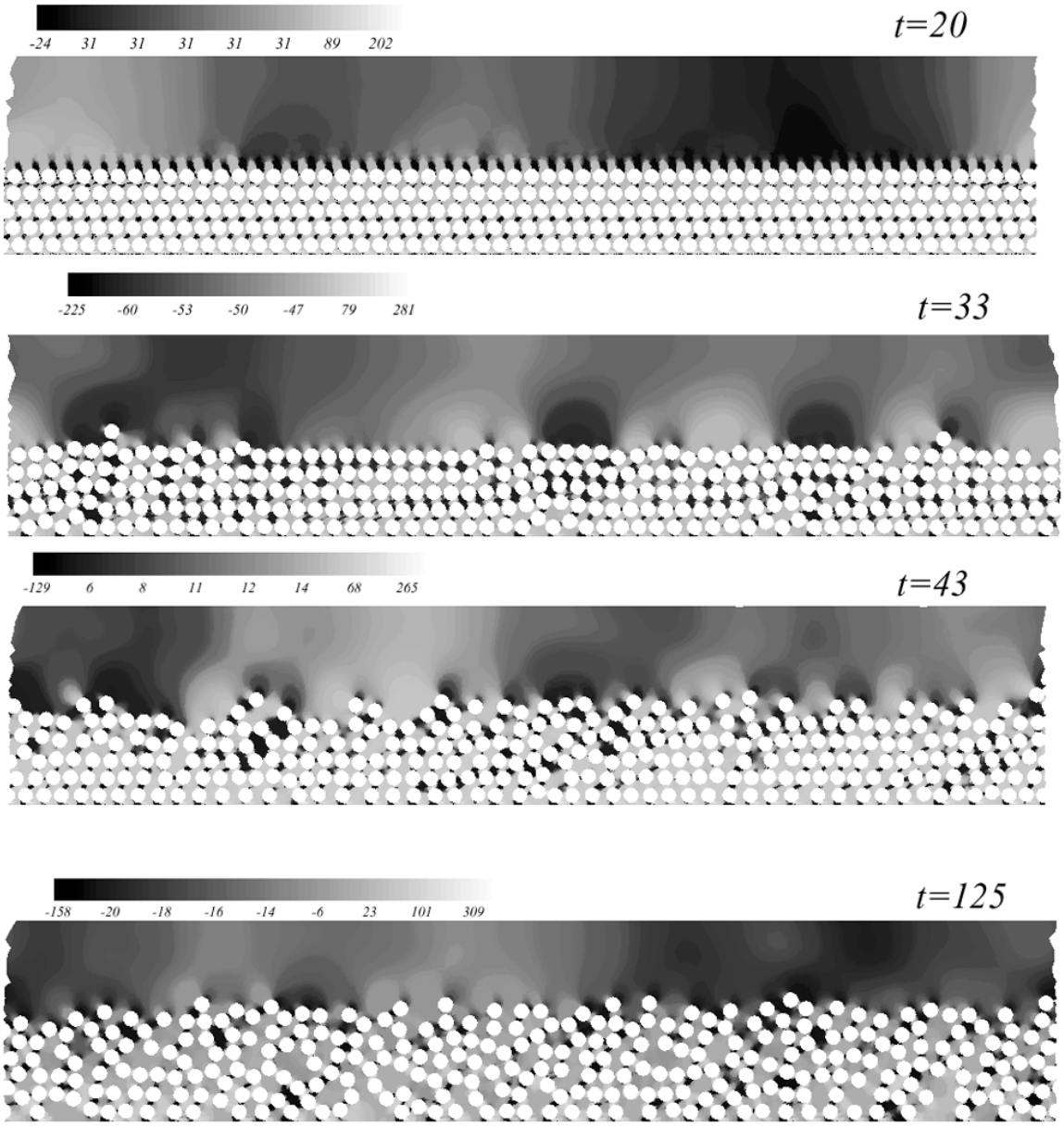

*Figure 5. Fluidization of 300 particles (*R = *16.2,* G = *0.61). The conditions are the same as in figure 4 except that the lift forces are greater leading to a more complete and faster fluidization.*

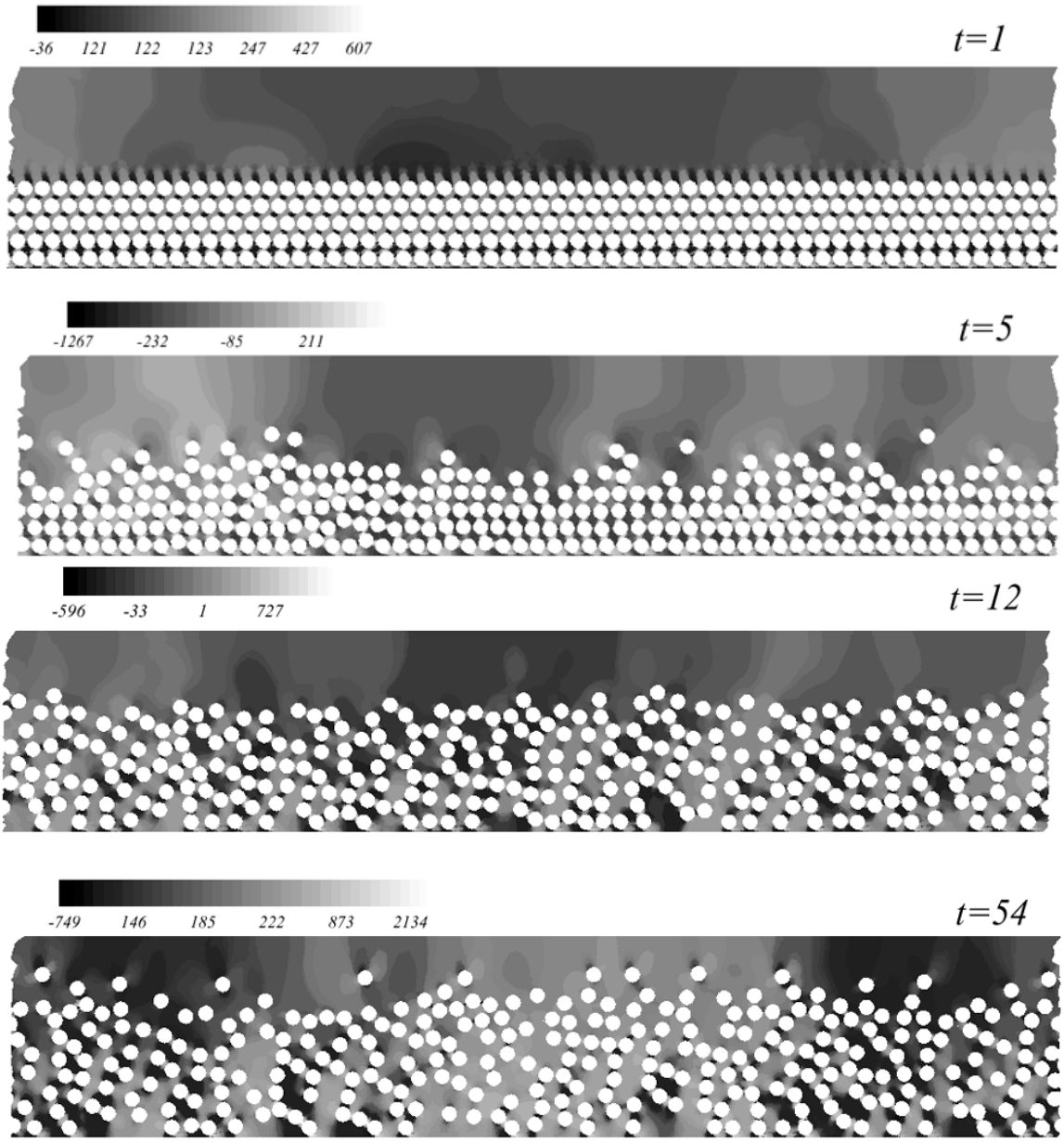

*Figure 6. Fluidization of 300 particles (*R = *60,* G = *0.16). The conditions are as in figure 4. The ratio* $\mathrm{R/G} = \dot{\gamma}_w^2 d \big/ \left(g\Delta\rho / \rho\right)$ *measures the ratio of lift to buoyant weight. Here the ratio is very large leading to fast and complete fluidization; the entire bed has eroded.*

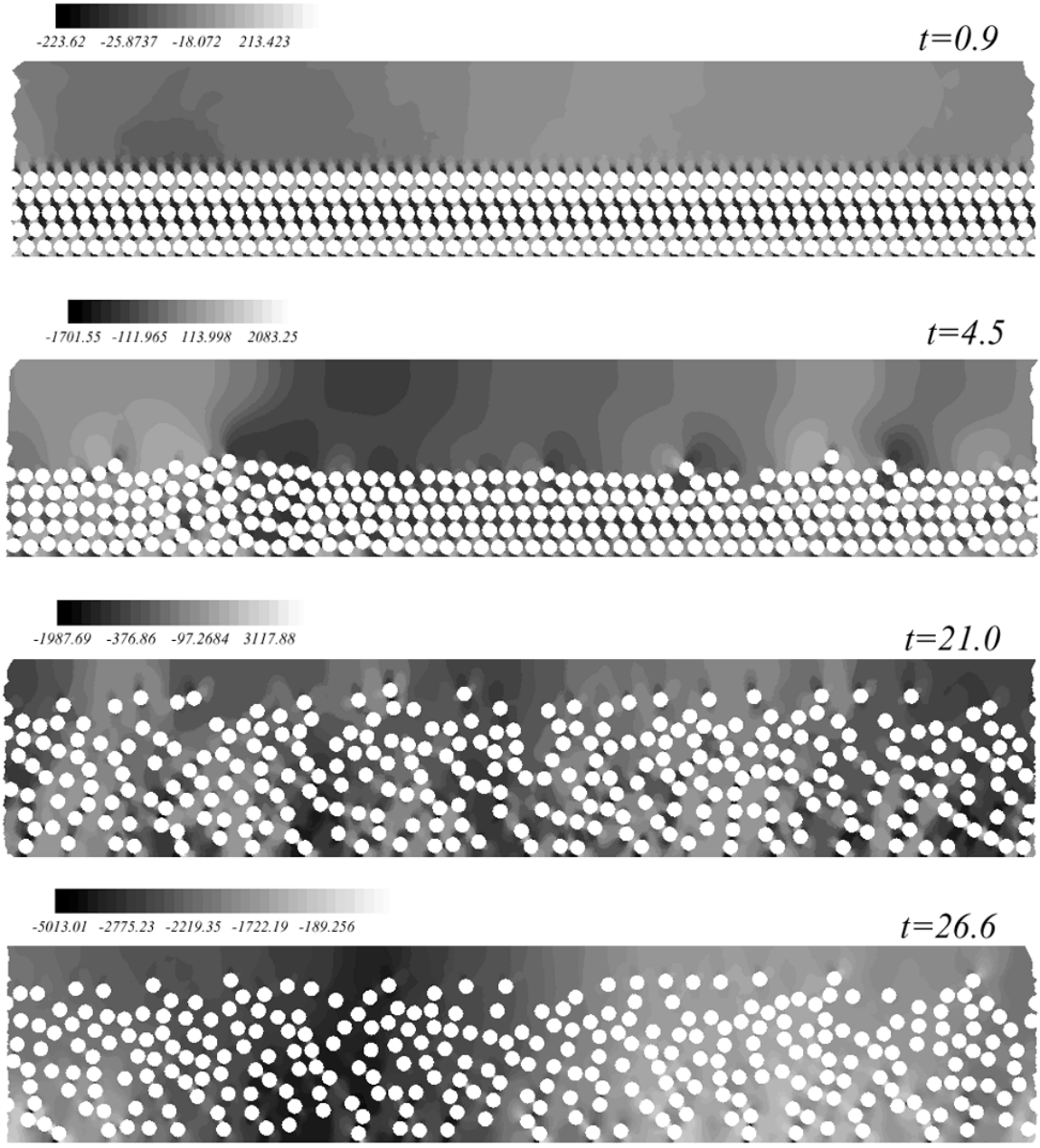

*Figure 7. Fluidization of 300 particles (*R *= 120, G = 0.08). The conditions are the same as in figure 4 and figure 6 but the ratio of lift to buoyant weight is greater and the fluidization is faster and the particle mass center rises higher than in the previous figures.*

In figures 8 and 9 we plotted the distribution of pressures at an early and late time when $R = 120$, $G = 0.08$. The figures show that the vertical stratification of pressure at an early time evolves to waves of pressure which are associated with propagating number density or voidage waves.

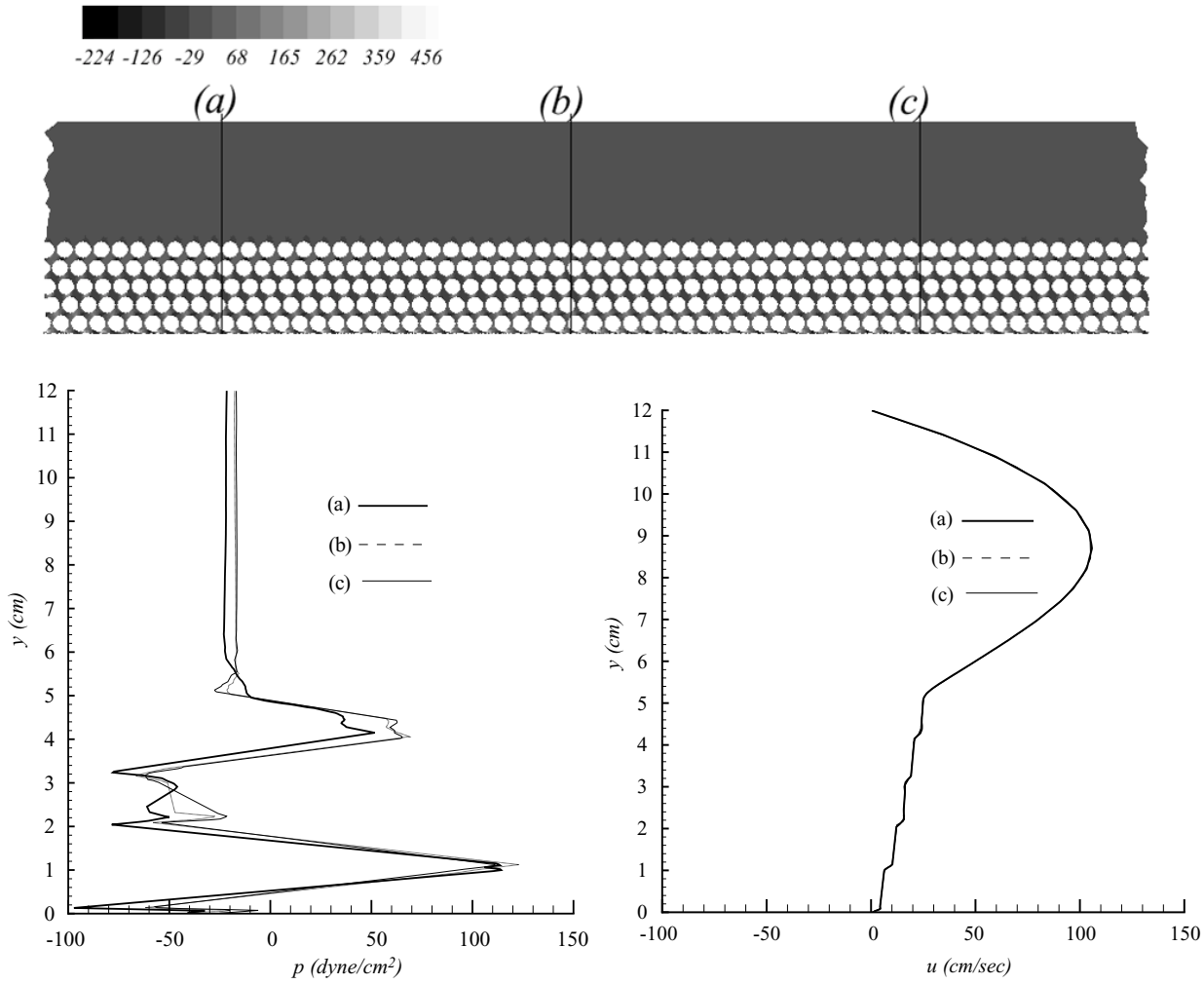

Figure 8. Distribution of dynamic pressure p *and streamwise velocity* u *at an early time (*t *= 0.9 sec) when* R *= 120,* G *= 0.08 (cf. Figure 7) at different cross sections of the channel. The dynamic pressure is stratified vertically but not horizontally. The rows of particles slide relative to one another moving like rigid bands separated by liquid.*

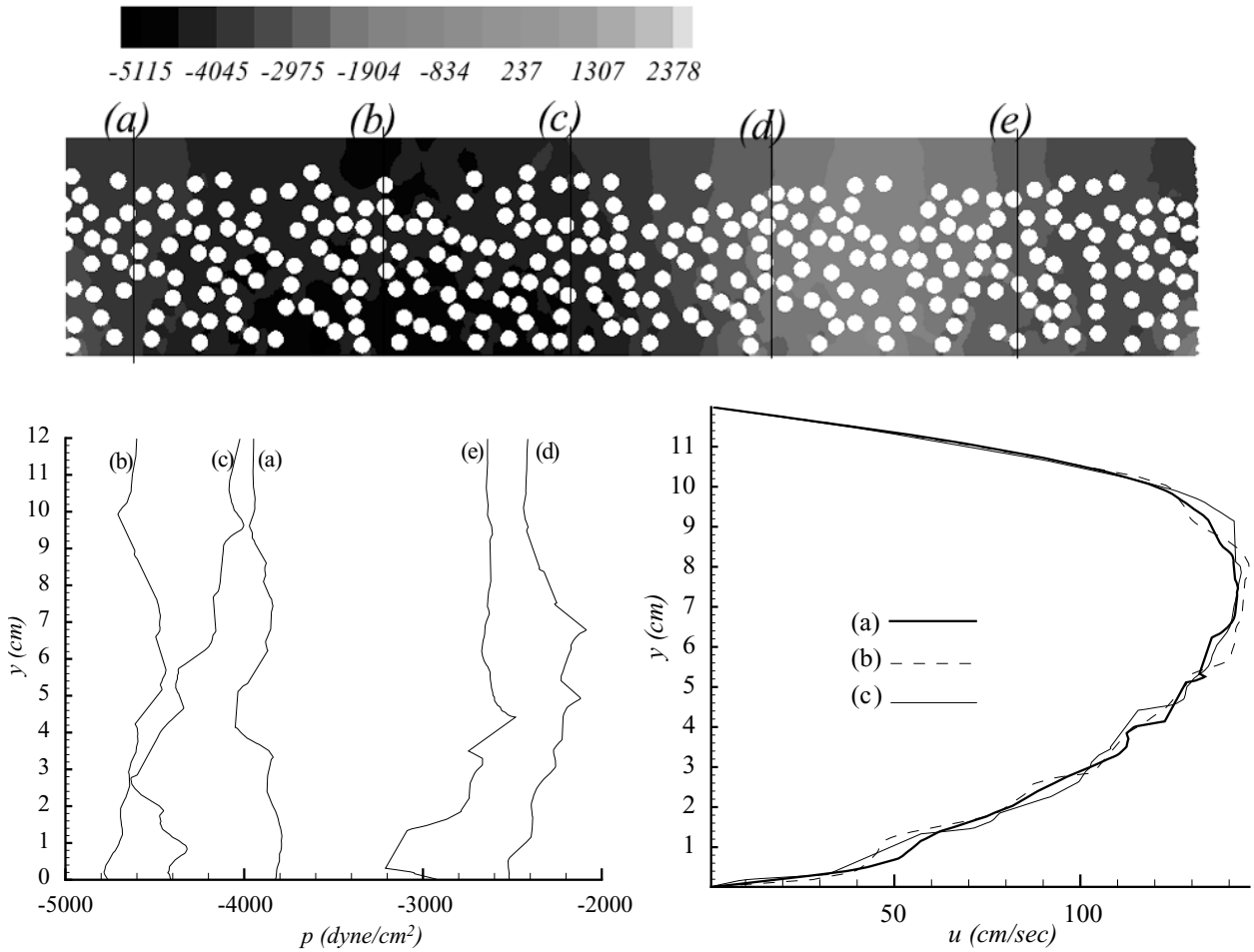

Figure 9. Distribution of dynamic pressure p *and streamwise velocity* u *after full fluidization (*t *= 27 sec) when* R *= 120,* G*= 0.08. The pressure* p *is stratified horizontally and not vertically; pressure pulses propagate horizontally.*

▪ Case 2: η= 0.2 poise, R_G = 245

Figure 10 shows the height of the center of the gravity of the 300 particles as a function of $R = 6\overline{p}/\eta^2$. The interpretation of figure 10 is basically the same as figure 3. Average values of the bed height $\overline{H}$ cm, velocity $\overline{U}$ cm/sec, and angular velocity $\overline{\Omega}$ sec^{-1} at full fluidization are given in table 2. Snapshots of the evolution to full fluidization are shown in figures 11 and 12.

Table. 2 Data for the forward motion of a fluidized suspension of 300 particles after the bed has fully inflated and the average height $\overline{H}$ *of all particles has stopped increasing* $(\eta = 0.2)$. $\overline{H} = \overline{H}_o = 2.65d$ *at t=0.* $\overline{U}$ *and* $\overline{\Omega}$ *are the average velocity and angular velocity of the particles.*

R	G	$\overline{p}$	$\overline{H}$	$\overline{U}$	$\overline{\Omega}$
45	5.44	0.3	2.64	3.17	0.42
150	1.63	1.0	3.30	10.75	1.25
300	0.82	2.0	3.82	22.98	2.43
450	0.54	3.0	4.75	34.15	2.02

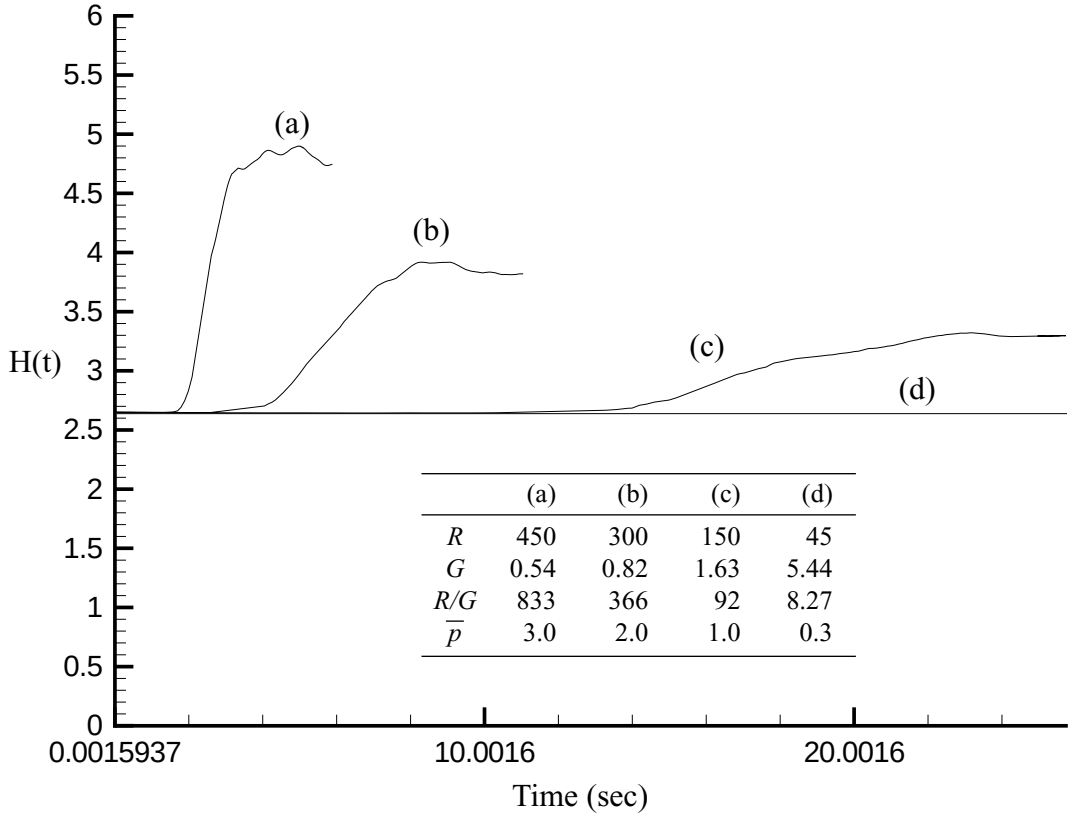

Figure 10. Rise curves for the center of gravity of 300 circular particles fluidized by lift (fluid viscosity = 0.2, RG = 9.81/η^2 *= 245.)* $\overline{p}$ *is in dyne/cm*^{2}*. The bed is fully fluidized when the rise curves level off. The time to full fluidization is longer when the Reynolds number is smaller. The time to full fluidization is faster when* η *= 0.2 than when* η *= 1 (figure 3). The time is scaled down by 5 and the center of gravity of the particles will eventually rise when* $(R, \overline{p}) = (45,0.3)$.

The description in the caption of figure 4 applies also to figures 11 and 12 except that the particles are more mobile when the viscosity of the fluid is smaller. The particle laden region at t = 25 sec in figure 11, and t = 1.98 in figure 12 is separated from the particle free region by an "interface" which propagates like an interfacial wave. This interface disappears at a higher R = 450, figure 12 for t > 2.7 sec, because the stronger lift forces push wave crests into the top of the channel; however, the pressure and associated void fraction wave persists.

The pressure wave at t_0 = 4.204 sec for the case (η = 0.2, R = 450) in figure 12 is analyzed in figure 13. The period of this wave is T = 0.56 sec and its wavelength is 16 cm. The pressure wave is associated with a wave of solids fraction which could also be described as the passage of internal wave crests and troughs.

Figures 14 and 15, like figures 8 and 9, show the evolution of dynamic pressure from an essentially vertical stratification at early time (t = 0.1 sec) to propagating horizontal waves in the fully developed suspension at t = 4.95 sec.